Millimeter Wave Spread in Delay and Azimuth for Small Cell Propagation Channel at 60 GHz

Mir Ghoraishi[†], Sana Salous[§], Yuteng Gao[‡], Rahim Tafazolli[†]

[†] 5G Innovation Centre, University of Surrey, UK, Emails: {m.ghoraishi, r.tafazolli}@surrey.ac.uk
[§] University of Durham, UK, Email: sana.salous@durham.ac.uk
[‡] School of Electronics and Information, Northwestern Polytechnical University, Xian, China

***Abstract*—The millimeter wave channel at 60 GHz for line-of-sight small cell scenarios was examined through analysis of the measured data using a wideband channel sounder. Full polarimetric directional data obtained at 3 different locations for which the emulation of small cell base-station (transmitter) antenna is at the height of 5 m from the ground floor, where the user-equipment (receiver) is located at 10 locations with different distances between 5 m to 50 m from the base-station. The base-station antenna is as wide to illumitate the small cell whereas at the user-equipment side a 5° beamwidth narrowbeam antenna is used to obtain the directional channel impulse response with high resolution in azimuth-of-arrival and delay. The analysis of the measured data confirms the dominance of the line-of-sight component with small root-mean-squared (RMS) values for delay. Few dominant scatterers can be observed at each environment which increase the delay and angular spread values.**

I. Introduction

Mobile communications industry is looking at new spectrum bands, in the range of up to 100 GHz to be able to reach the fifth generation (5G) mobile system requirements. It is known that there are available spectrum at some of these millimeter bands to employ wide bandwidth channels, however accurate radio wave channel models have to be produced yet. In this regard, there has been various efforts to analyze the millimeter wave radio channel through measurements and by the extrapolation of the sub-6 GHz radio channel knowledge [1].

A survey of state-of-the-art millimeter wave channel measurement and modeling for mobile communication systems can be found in [2]. The 60 GHz band which is the topic of this paper has been mostly studied for indoor scenarios so far. This might have been due to high Oxygen loss at this band and the existing wireless HD technologies (WiGig) which primarily targets indoor coverage [3]. Nevertheless the 60 GHz unlicensed band exhibits a great potential for backhaul and small cell radio access, and thus the propagation channel for these scenarios need to be carefully investigated. There are few outdoor studies on the 60 GHz radio channel, where the earliest studied street microcell at 59 GHz and showed that the delay spreads are less than 20 ns sor such scenarios [4]. Similar results were obtained for a measurement campaign with 200 MHz bandwidth and concluded that there are few multipath components in street microcell scenarios [5]. On the other hand, it was confirmed that the line-of-sight component is dominant in the street microcell, although the ground reflection component can be significant too when the line-of-sight is blocked at larger distances [6] . The study of path loss for outdoor 60 GHz scenarios suggests a path-loss exponent of around 2 [5], and [6].

This paper aims to provide further data on the radio channel of small cell at 60 GHz. For this purpose a measurement campaign was performed on the campus of Durham University, UK. The scenario of measurement is outdoor line-of-sight small-cell. The ultimate purpose of this measurement is to obtain a reliable set of data with appropriate resolution for proposing a wideband, directional channel model for 5G small-cell scenarios. Details of measurement description, parameters as well as the analysis of the measurement data are presented below.

II. Scenario and Measurement

This campaign aims to investigate the characteristics of outdoor small-cell propagation channel at 60 GHz. The schematic of the measurement setup is illustrated in figure 1 which represents small-cell scenario with the base-station (transmitter) antenna at both polarizations mounted on a mast at a height of 5.0 m. The scenario is line-of-sight which means the user-equipment (receiver) antenna mounted on the measurement trolley is in the line-of-sight of the transmit antenna. The channel sounder used in the measurements has two transmitters and two receivers with a programmable bandwidth up to 6 GHz [7]. The parameters of the measurements reported in this paper are listed in Table 1 with the setup as follows:

1) The sounder was configured to transmit on the two channels with horizontal and vertical polarizations with 2.2 GHz bandwidth to give 0.45 n time delay resolution. The transmit power is 7 dBm on each transmitter.
2) Base-station emulation: As transmitter, the antennas at both polarizations are installed at a height of 5.0 m from the ground by using the measurement mast. Directional antennas with 18 dB gains are used with an appropriate tilt to cover the small-cell environment. The directionality is wide enough to cover the desired area in the small-cell with no compromise to gain.
3) User-equipment emulation: As receiver, user-equipment emulator setup is placed on the measurement trolley assisted with rotating table. The antenna height is set

TABLE I
SPECIFICATIONS OF EXPERIMENT

f_c	60 GHz
RF bandwidth	2.2 GHz
Delay resolution	0.45 ns
Transmit power	7 dBm
Transmit antenna gain	18 dB
Receive antenna gain	36 dB
Receive antenna beamwidth	5°
Azimuth-of-arrival resolution	5°

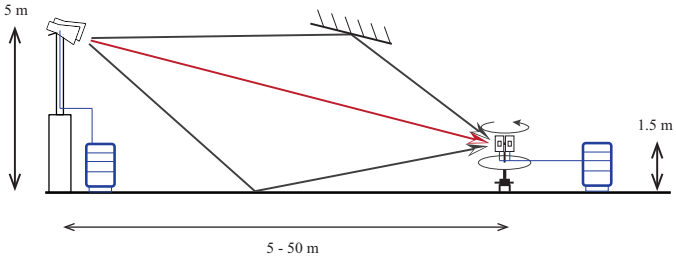

Fig. 1. Schematic diagram of the measurement scenario.

1.70 m from the ground, at around the height of a typical user. Highly directional antenna with 5° with 36 dB gain is used to capture directional received signal with required angular resolution, and a rotating table is used to scan the azimuth with a rotation increment step of 5°. This gives a total of 73 azimuth directions for each location.

4) Thus to capture the received signal at both polarization, two rounds of measurements are necessary, i.e. user-equipment side scans the azimuth two times at each location.

A. Environment

Measurements were performed at 3 small cells (base-station setup at 3 locations). The locations of the base-station and user-equipment at the measurement are specified in the map of figure 2. The environment of the measurement at route 1 is displayed in figure 3. Routes 2 and 3 are more or less similar in terms of surrounding building heights, width of the street and density of street furniture, etc.

Maximum distance of user-equipment to the base-station (measurement range) in all measurements is 50.0 m. Where for each base-station location, the user-emulator is placed at least at 10 locations of the small-cell (roughly covering the 10.0 to 50.0 m distance from the base-station on each route). The number of measurement locations in each cell was set to capture an appropriate statistical sample of the propagation channel.

The scenario and environment was arranged in a way to ensure (within the possible range) the stationarity of the channel. No vehicular traffic during the measurement existed and pedestrian traffic was minimized. This was important since at the frequency band of measurements any movement of

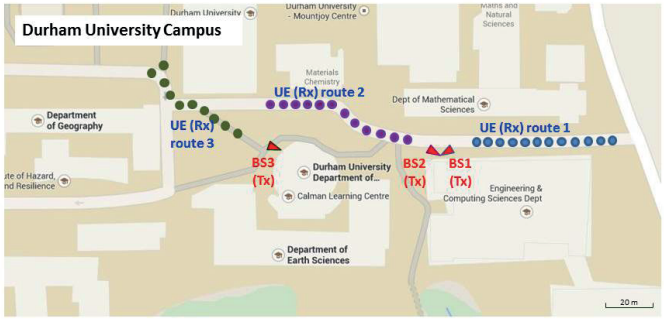

Fig. 2. Measurement routes on campus, Durham University.

Fig. 3. Environment of the route 1.

objects with normal sizes might cause significant change in the channel.

For each base-station location 10 UE locations were measured with both transmit polarizations V and H and repeated to obtain the full polarimetric channel parameters.

III. MEASUREMENT DATA ANALYSIS

All required calibrations were performed and the channel impulse responses at each direction were averaged over all snapshots to maximize the signal-to-noise ratio of the measured data. The measured channel impulse responses for full polarimetric combination (V/H to V/H) are derived with a delay resolution of 0.45 ns and azimuth angle of arrival resolution of 5°. In the preprocessing of the data, the average impulse responses over each direction on the azimuth are derived and then the directional delay power profile is normalized at each point to the maximum received power at that point. This normalization is necessary since the absolute received power (equivalently absolute path-loss) is not knowable because the effective antenna gain at the direction of the line-of-sight component is unknown.

The polarimetric power delay profiles show the spread of the channel in specific direction for which the scatterers in the delay and angular domains can be identified. Figures 4 and 5 display the normalized power delay profile for vertical-to-vertical (VV) and horizontal-to-horizontal (HH) scenarios respectively. It is observed that components as strong as 10 dB lower than the strongest signal can be observed with

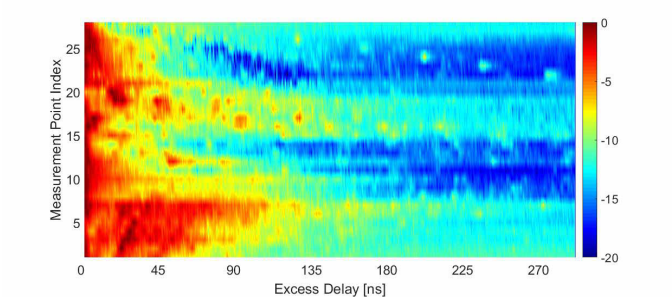

Fig. 4. Normalized power delay profiles [dB], VV scenario .

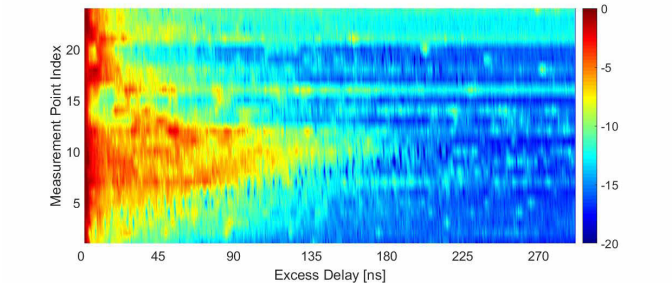

Fig. 5. Normalized power delay profiles [dB], HH scenario .

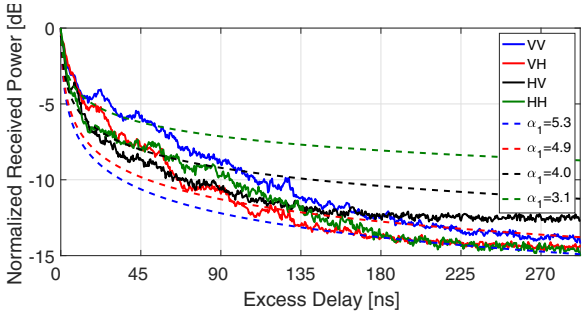

Fig. 6. Path loss for all polarization scenarios and the fitted equation.. .

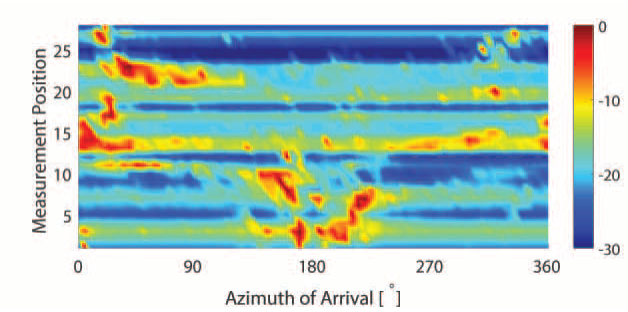

Fig. 7. Directional received power normalized [dB], VV scenario .

delays up to 90 ns. Normalized received power averaged over all measurements points for all polarization scenarios are presented in figure 6. This figure shows that the VV scenario has stronger delayed components compared to other scenarios. This indicates that major scatterers in these scenarios favor the VV interactions. Figure 6 also include fitting curves to model the multipath decaying in such scenarios. Here an exponential decaying model for the average received power across the delay is used as

$$P_i = \alpha_0 - 10\alpha_1 \log \tau_i \tag{1}$$

with P_i to be the average received power at delay τ_i, and α_0 and α_1 are model parameters. To fit this model, four values of α_1 are being used and displayed in figure 6. It is noted that figure 6 shows the average (over all measurement positions) multipath spread for each polarization scenario.

Figures 7 and 8 show the polarimetric normalized directional received power at each measurement point only for VV and HH scenarios. As it is expected for the line-of-sight scenario, these results show the dominance of the line-of-sight component in all measurement points.

A. RMS delay spread

The RMS delay spread of the channel at all polarizations is calculated as

$$\tau_{\text{rms}} = \sqrt{\frac{\sum_i P_i(\tau_i - \tau_{\text{rms}})^2}{\sum_i P_i}} \tag{2}$$

where τ_i indicates the delay of the ith multipath with received power P_i, and τ_{rms} is the average delay of the multipath.

First, the polarimetric-directional RMS delay profile at each measurement point for the VV and HH scenarios are shown in figures 9 and 10. A threshold of -20 dB compared to the strongest received signal at each measurement position was used to take into account multipath with significant power. A comparison of directional RMS delays vs directional received power, i.e. figures 7 and 8 compared to figures 9 and 10 when the line-of-sight component or a strong scatterer exist, the RMS delay values are low, i.e. around 20 ns.

Over all measurement positions and routes, figure 11 presents the RMS delay spread of the channel for all polarization scenarios. It is observed that the delay values for the HH scenario shows more spread compared to other polarization scenarios. It can be said that the nominal value of the delay spread for %50 CDF is around 20 ns, and for %90 is more than 50 ns. However in general for the scenarios under investigation at 60 GHz where only few scatterers may exist in the channel, the spread of the channel across delay and direction of

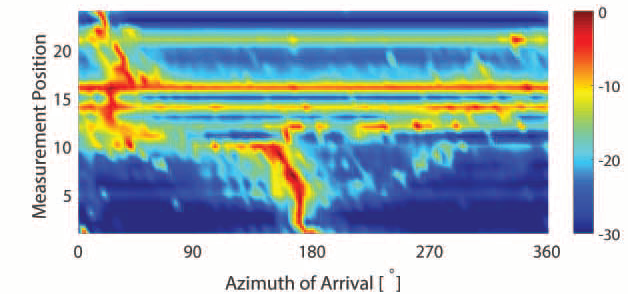

Fig. 8. Directional received power normalized [dB], HH scenario .

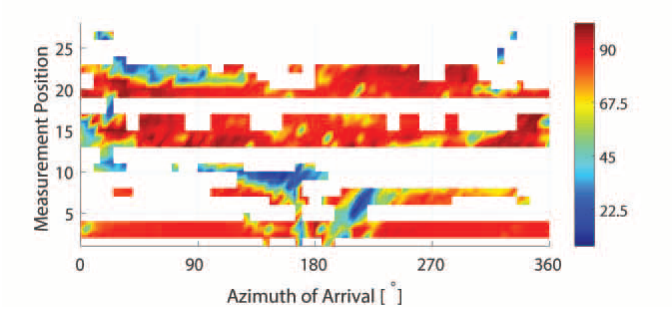

Fig. 9. Directional received signal RMS delay [ns], VV scenario.

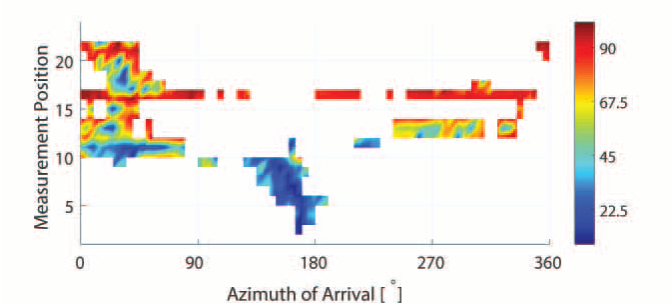

Fig. 10. Directional received signal RMS delay [ns], VV scenario.

arrival heavily relies on the existence and distribution of these scatterers.

IV. Conclusion

A radio channel measurement campaign at 60 GHz for line-of-sight small cell scenario and its data analysis is reported in this paper. The measurement is wideband, directional and fully polarimetric using a channel sounder with 2.2 GHz signal, high gain directional antenna with 5° beamwidth, and various polarization scenarios by using both polarization antenna at the transmitter and changing the horn antenna orientation at the receiver end. The measurement scenario includes small cell base-station emulation (transmitter) at 3 different locations, on campus, Durham University, where the antenna is installed at the height of 5 m from the ground floor. At the other end of the link, the user-equipment (receiver) at the height of 1.6 m from the ground floor, is located at 10 locations with different distances between 5 m to 50 m from the base-station.

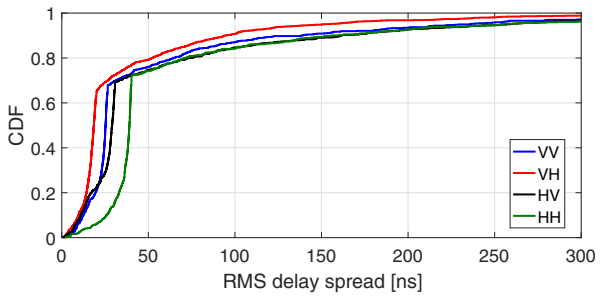

Fig. 11. CDF of the RMS delay spread over all routes [ns].

The spread of the received signal along azimuth-of-arrival and delay was investigated, where it is observed that other than possibly few main scatterers at each measurement point, the line-of-sight component is dominant. The RMS delay spread of the directional received signal shows a small delay spread around the dominant received signal components. The existence of small number scatterers in the channel can cause significant change in the delay and angular spread values. This can hint the effectiveness of sight-specific channel models for such scenarios compared to other approaches.

V. Acknowledgment

We would like to acknowledge the support of the University of Surrey 5GIC (http://www.surrey.ac.uk/5gic) members for this work.

References

[1] METIS2020, Deliverable D1.4 v3, METIS Channel Model, July 2015.
[2] T. Rappaport, G. MacGartney, M. Samimi, S. Sun, "Wideband Millimeter-Wave Propagation Measurements and Channel Models for Future Wireless Communication System Design,"' *IEEE Trans. Commun.*, Vol. 63, No. 9, Sept. 2015.
[3] C. Hansen, "WiGiG: Multi-gigabit wireless communications in the 60 GHz band, *IEEE Wireless Commun.,* Vol. 18, No. 6, pp. 67, Dec. 2011.
[4] G. Lovnes, J. Reis, and R. Raekken, "Channel sounding measurements at 59 GHz in city streets, *in Proc. of IEEE Int. Symp. Personal, Indoor, Mobile Radio Commun. (PIMRC),* Sep. 1994.
[5] P. Smulders, L. Correia, "Characterisation of propagation in 60 GHz radio channels, *Electron. Commun. Eng. J.,* Vol. 9, No. 2, Apr. 1997.
[6] W. Keusgen, R. Weiler, M. Peter, M. Wisotzki, and B. Goktepe, "Propagation measurements and simulations for millimeter-wave mobile access in a busy urban environment, *in Proc. 39th IRMMW-THz,* Sep. 2014.
[7] S. Salous, S. Feeney, X. Raimundo, A. Cheema, "Wideband MIMO channel sounder for radio measurements in the 60 GHz band," *IEEE Trans. on Wireless Commun.,* 15(4), pp. 2825-2832, 2016.